CH-99-1-3

Predicting the Position of the Smoke Layer Interface Height Using NFPA 92B Calculation Methods and a CFD Fire Model

William N. Brooks, P.E.

ABSTRACT

NFPA Standard 92B presents computational methods for determining the position of a smoke layer in a large-volume space. Although NFPA 92B is a guide to smoke management design, the methods have been adopted, with certain modifications, by model building codes and are mandated for use in atriums and large-volume spaces. This paper makes use of a recently developed CFD fire model to assess the NFPA 92B calculation methods. A total of 13 simulated tests were conducted. Results suggest that the NFPA 92B Equation 9 method may not predict the fastest filling of an enclosure within the range of aspect ratios provided in NFPA 92B.

INTRODUCTION

Prediction of smoke layer interface heights in large-volume spaces is essential to certain building fire-protection and life-safety strategies. Predicted positions of the smoke layer interface height can be applied to egress design or to property conservation.

Figure 1 depicts the development of the fire plume, the formation of the smoke layer as the fire plume radiates outward to the surrounding walls, and the smoke layer descent. Figure 2 illustrates a cross-sectional view of an atrium with a descending smoke layer. The terms used are defined as follows:

H	=	highest point of smoke accumulation
Z	=	height of smoke layer interface
Z_{CR}	=	critical (design) height of smoke layer interface
z_l	=	limiting elevation (defined as the height of the luminous flame)

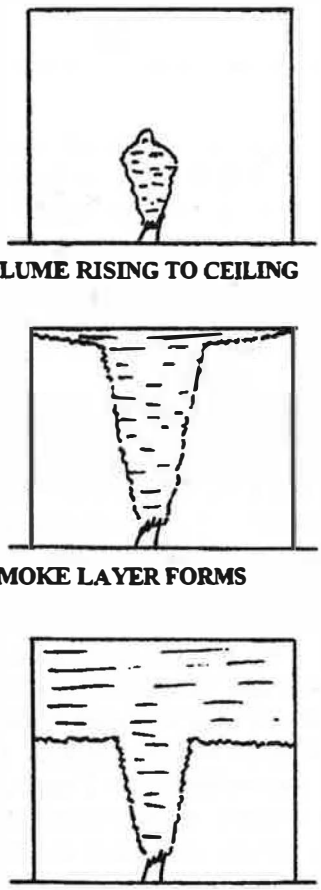

Figure 1 *Smoke filling of atrium space: (a) plume rises to ceiling; (b) smoke layer forms; (c) smoke layer descends.*

William N. Brooks is fire protection department manager, Peter F. Loftus Division, Eichleay Engineers, Inc., Pittsburgh, Pa.

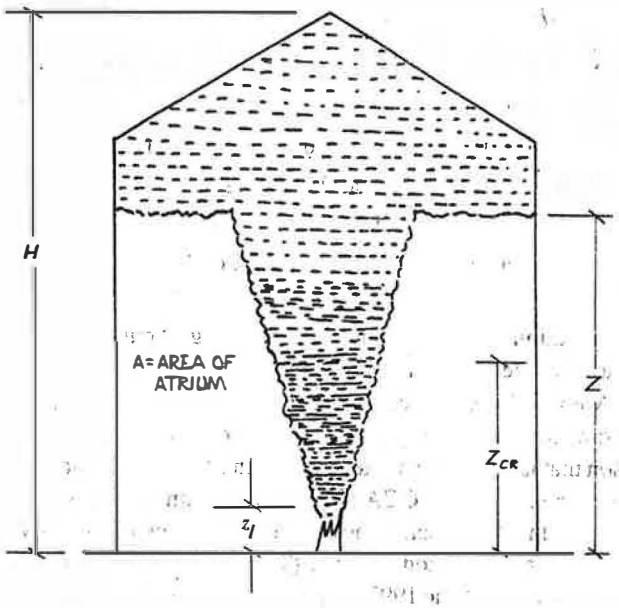

Figure 2 H—Highest point of smoke accumulation; Z—Height of smoke layer interface; Z_{cr}—Critical (design) height of smoke layer interface; z_l—Limiting elevation (height of luminous flame).

A = Horizontal cross-sectional area of atrium

Aspect ratio = A/H^2

NFPA Standard 101 (Life Safety Code) and the *1996 BOCA National Building Code* (BOCA 1996) use the NFPA Standard 92B methodology in a manner that links the position of the smoke layer at a particular time to the requirement for a smoke management system (see BOCA Code, Section 922.2, and NFPA 101, Section 6-2.4e). The *Uniform Building Code* (ICBO 1997) does not utilize a time consideration in its large-volume design criteria. Instead, a smoke exhaust system must be capable of maintaining an interface height 3.1 m (10 ft) above the highest walking surface in the smoke zone (see ICBO Code, Section 905.5.2.1). Therefore, the time of smoke layer descent is a critical factor in NFPA 101 and the BOCA Code design but is not relevant to ICBO Code design.

A previous paper by the author (Brooks 1997) showed that the two design methods in the BOCA Code produce results that va y significantly. In fact, an example in the *1993 Commentary* (BOCA 1993) was used to illustrate that a smoke management system is requiredwh en the calculation method for regular spaces is used, while a smoke management system is not required when the calculation for irregular spaces is used.

A large eddy simulation, computational fluid dynamics (LES CFD) model (McGrattan et al. 1998) is used in an attempt to reconcile the differences among a number of calculation methods.

METHODOLOGY

Four calculation methods are used to predict the position of the smoke layer interface in a total of 13 simulated test cases using steady-state heat release rate fires.

- Method 1—NFPA 92B, Equation 9 (calculation method for regular spaces described in the 1996 BOCA Code)
- Method 2—NFPA 92B, Equation A-26
- Method 3—NFPA 92B, Equations 14 and 15, adjusted for smoke layer temperature
- Method 4—Large eddy simulation CFD model

Table 1 is a list of the individual test cases. With the exception of Test No. 10, the selected aspect ratios are consistent with NFPA 92B and the 1996 BOCA Code. Heat release rates include the range of fire sizes that are mandated for use by the BOCA Code (2110, 4640 kW) and the ICBO Code (5275 kW). Selected areas represent the author's opinion as to where the design methods will be most widely utilized.

Test No. 10 represents a more slender aspect ratio that is not contemplated by NFPA 92B or the 1996 BOCA Code. It has been included for sensitivity purposes.

All of the cases assume a flat horizontal ceiling and a uniform square horizontal cross-sectional area with vertical sides.

CALCULATION METHODS

Methods 2 and 3 can be defined as zone models, which predict well-defined smoke layer positions at any given time and distinct differentiation between the smoke layer and the clear air below. Smoke layer interface positions are assumed

TABLE 1a
Selected Test Cases
(Selected Test Conditions [SI Units])

Test No.	Aspect Ratio	Area (m^2)	Height (m)	Heat Release Rate (kW)
1	10	9303	30.5	2110
2	0.9	9290	101.6	2110
3	0.9	9290	101.6	4640
4	10	922	9.6	2110
5	0.9	927	32.1	2110
6	0.9	927	32.1	4640
7	14	941	8.2	4640
8	14	4688	18.3	4400
9	14	9391	25.9	4400
10	0.5	929	43.1	4640
11	14	26007	43.1	15718
12	0.9	1672	43.1	9693
13	0.9	1672	43.1	544

TABLE 1b
Selected Test Conditions
(Selected Test Conditions [IP Units])

Test No.	Aspect Ratio	Area (ft^2)	Height (ft)	Heat Release Rate (Btu/sec)
1	10	100,000	100	2000
2	0.9	100,000	333	2000
3	0.9	100,000	333	4400
4	10	10,000	31.5	2000
5	0.9	10,000	105	2000
6	0.9	10,000	105	4400
7	14	10,000	27	4400
8	14	50,000	60	4170
9	14	100,000	85	4170
10	0.5	10,000	141.5	4400
11	14	280,000	141.5	14,900
12	0.9	18,000	141.5	9,200
13	0.9	18,000	141.5	520

to be level and to fill atrium volumes much like an inverted version of water filling a bucket.

Method 1 is also a zone model, with the exception that it does not define the position of the smoke layer interface. Instead, the results of this calculation method are to be viewed as the first indication of smoke, or the beginning of the transition between clean air and contaminated air (NFPA 92B, Figures 1 through 4 and accompanying definitions). It does not assess the quality of the environment at the transition point, only that this is the point where the transition begins to occur.

Method 4 is the LES CFD model, relying on a much more precise calculation technique to establish the characteristics of the atrium environment. This method is able to define the position where temperature change occurs as a result of plume interaction with the ambient air.

There is no standard to define the position of the smoke layer interface. A number of papers address this topic, and a number of methods are proposed (Chow 1995; Söderbom 1992; He et al. 1998) Experimental programs use a combination of visual observations, thermocouple trees, and light obscurat on meas rement equipment to record the position of the smoke layer at any given time (Yamana and Tanaka 1985). Therefore, the results of the calculat ons will vary in that they may be predicting different phenomena. That is, Method 1 is predicting "first indication of smoke," Methods 2 and 3 are predicting similar smoke layer positions, and Method 4 is much like visual observations that would be made in an experimental program.

Method 1—NFPA 92B, Equation 9

The position of the smoke layer interface, Z, is predicted at any time using the following equation:

$$Z/H = 1.11 - 0.28 \ln [(tQ^{1/3}/H^{4/3})/(A/H^2)] \qquad (1)$$

where

Z = height from the floor to the smoke interface (m),
t = time for the interface to extend to Z (s),
H = height from floor to flat ceiling (m),
Q = steady-state heat release rate (kW),
A = horizontal cross-sectional area of the space being filled (m^2).

Equation 1 is a correlation, representing a "curve fit" of a limited number of fire tests (NFPA 1995).

Method 1 does not readily lend itself to a hand-calculated solution for t, given a particular value of Z/H. It is for this reason that it would most often be used in a "pass-fail" manner, as presented by the BOCA Code to determine if the smoke layer interface has reached the critical height (design objective level) in a given period of time. (The *1996 BOCA National Building Code* and the 1997 NFPA *Life Safety Code* define this period of time as 1200 seconds.)

The usefulness of this method is presented by the *1996 BOCA National Building Code* as a single-point "test" to determine if the smoke layer interface has reached a given point (Z/H) in a defined time period. However, with some manipulation, the use of the method can be expanded to graphically plot the position of the layer at any given time.

Method 2—NFPA 92B, Equation A-26

The posit on of the smoke layer interface, Z, is predicted at any time using the following equation:

$$Z/H = \{1 + [2k_v(tQ^{1/3}/H^{4/3})/3(A/H^2)]\}^{-3/2} \qquad (2)$$

where

Z = height from the floor to the smoke interface (m),
t = time for the interface to extend to Z (s),
H = height from floor to flat ceiling (m),
Q = steady-state heat release rate (kW),
A = horizontal cross-sectional area of the space being filled (m^2),
k_v = entrainment constant (use 0.064 $m^{4/3}/[s\text{-}kW^{1/3}]$).

Although Equation 1 is based on a curve fit of a number of fire tests, Equation 2, according to NFPA 92B, is a theoretically based equation for smoke filling "derived using the laws of conservation of mass and energy to determine the additional volume being supplied to the upper layer" (NFPA 1995, Appendix A-3-6.2.2).

Method 3—NFPA 92B, Equations 14 and 15, Adjusted for Smoke Layer Temperature

Basic Calculation Method. This method relies on an integrative approach that utilizes the following NFPA 92B plume mass flow rate correlations:

$$m = 0.071 Q_c^{1/3} Z^{5/3} + 0.0018 Q_c \text{ (NFPA 92B, Eq. 14)} \quad (3)$$

where

m = mass flow rate in plume at height Z (kg/s) and

Q_c = convective portion of heat release rate (kW),

where

$$Q_c = 0.7Q \quad (4)$$

and

$$m = 0.032 Q_c^{3/5} Z \text{ (NFPA 92B, Eq. 15).} \quad (5)$$

Equations 3 and 5 define a mass rate of smoke production. Equation 3 is to be used above the limiting elevation, calculated as follows:

$$z_1 = 0.166 Q_c^{2/5} \text{ (NFPA 92B, Eq. 13).} \quad (6)$$

Equation 5 is to be used at or below the limiting elevation.

Calculating the layer position is not straightforward as is the case with Methods 1 and 2. Method 3 requires the following iterative calculation procedure:

1. Calculate smoke mass production (m) using Equation 3 based on the ceiling height (H).
2. Convert smoke mass production (m) to smoke volume (V) using the following equation:

$$V = m/\rho \quad (7)$$

where

V = volumetric rate of smoke production (m^3/s) and

ρ = density of smoke (kg/m^3).

3. Distribute the smoke volume uniformly under the ceiling surface area (A) by dividing the smoke volume produced in the first time period (1 second) by the area of the atrium. This value becomes the incremental depth of the smoke layer.
4. Subtract the incremental smoke layer depth (dZ) from the ceiling height (H). The new height becomes the smoke layer interface height Z.
5. Calculate smoke mass production based on the smoke layer height (Z).
6. Repeat steps 2 through 5 until the smoke layer interface height descends to the limiting flame height (z_1). At this point, calculate the smoke mass production (m) using Equation 5.

The calculation method results in instantaneous distribution of smoke under the entire ceiling surface, without regard to transport time from the fire to the ceiling or without regard to the time required for the smoke movement horizontally under the ceiling surface. The method also fails to account for any horizontal entrainment that may occur as the smoke moves radially outward from the point where the plume centerline impinges on the ceiling.

Smoke Layer Temperature Correction

NFPA 92B provides no guidance regarding the use of this calculation method. The 1996 BOCA Code *Commentary* illustrates the iterative nature of the calculation but fails to adjust the volume of smoke production based on a smoke density correction. As reported previously (Brooks 1997), the BOCA Code irregular ceiling calculation method is based on smoke density at 21°C (70°F). Therefore, the resulting calculations will represent the slowest filling of the volume (i.e., smoke with the greatest density will occupy the smallest volume per kg).

In order to determine the sensitivity of the calculation method to smoke density, the smoke layer temperature is assumed to be uniform and equal to the average temperature of the plume centerline.

Adjusting the layer temperature will result in a decrease in smoke density and will increase the volume of smoke produced. The increased smoke volume will mean faster filling of the atrium.

For each test case, an average plume temperature is calculated using the following method:

1. Calculate the plume centerline temperature at the ceiling of the atrium and at the fire's limiting elevation (Equation 6):

$$T_{CL} = T_A + 25(Q_c^{2/3}/(Z-Z_0)^{5/3}) \text{ (Klote 1994)} \quad (8)$$

where

T_{CL} = plume centerline temperature (°C),

T_A = ambient temperature (21°C),

Q_c = convective portion of heat release rate (kW) (Equation 4),

Z = smoke layer interface height,

Z_0 = virtual origin.

For the atrium heights and heat release rates considered in this analysis, the virtual origin will be assumed to be at floor level.

2. Calculate average plume centerline temperature:

$$T_{AVE} = (T_H + T_1)/2 \quad (9)$$

where

T_{AVE} = average plume centerline temperature (°C),

T_H = plume centerline temperature at height H,

T_1 = plume centerline temperature at limiting elevation.

3. Calculate smoke density, using the average plume temperature:

$$\rho = p/RT \quad (10)$$

where

p = absolute pressure (101,325 Pa),

R = gas constant (J/kg K),

T = absolute temperature (K) = 273 + T_{AVE}.

4. The value for Equation 10 is inserted in Equation 7 and remains constant for the entire calculation period.

Method 4—Large Eddy Simulation CFD Model

The large eddy simulation CFD model (McGrattan et al. 1997) has been developed in conjunction with National Fire Protection Research Foundation at the National Institute of Standards and Technology. The model is seen as a valuable tool to reduce the overall costs of fire experiments by developing computational methods to predict fire phenomena. In addition to predicting and evaluating experimental results, the model is able to assist in planning experimental programs.

For this analysis, the LES CFD model is being used in place of 13 fire experiments. While the validation of the model is still in process, its use appeared to present an interesting opportunity to simulate fire conditions in order to compare the results from the three zone models to the LES CFD model.

The LES CFD model predicted the position of the smoke layer interface in each of the 13 cases. Since there is no mathematically defined method to determine the smoke layer interface position, the LES CFD modeler visually observed the simulated filling of the atrium enclosures. In a sense, the observation of the smoke layer interface descent using the LES CFD model is somewhat similar to observing an actual test.

Figure 3 illustrates the differences among observed data in a fire experiment (Yamana and Tanaka 1985). The test data represent the filling of a 24 m (78.7 ft) by 30 m (98.4 ft) by 26.3 m (86.3 ft) high enclosure. The aspect ratio (A/H^2) is 1.04. No mechanical ventilation is used during the test. The fire has a steady-state heat release rate, reported to be 1300 kW (1232 Btu/s). Note the differences among the photometer, thermocouple, and visual observations of the smoke layer interface position as it descends. Also note the linear nature of the descent as the interface descends below the 7 m (23 ft) height, corresponding to Z/H = 0.26. The dashed line represents the Yamana/Tanaka predicted filling. Figure 3 most closely represents Test 5 presented in this discussion.

CALCULATION RESULTS

Figure 4 illustrates predicted volume filling for each of the 13 tests. In this figure, the Method 3 calculations were performed without layer temperature correction. Note the

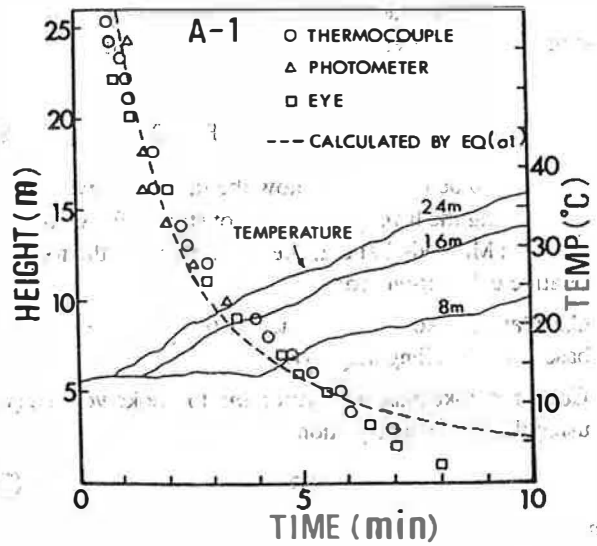

Figure 3 Yamana/Tanaka experimental results. Aspect Ratio = 1.04, H = 26.3 m (86.3 ft); Heat Release Rate = 1300 kW (1232 Btu/s).

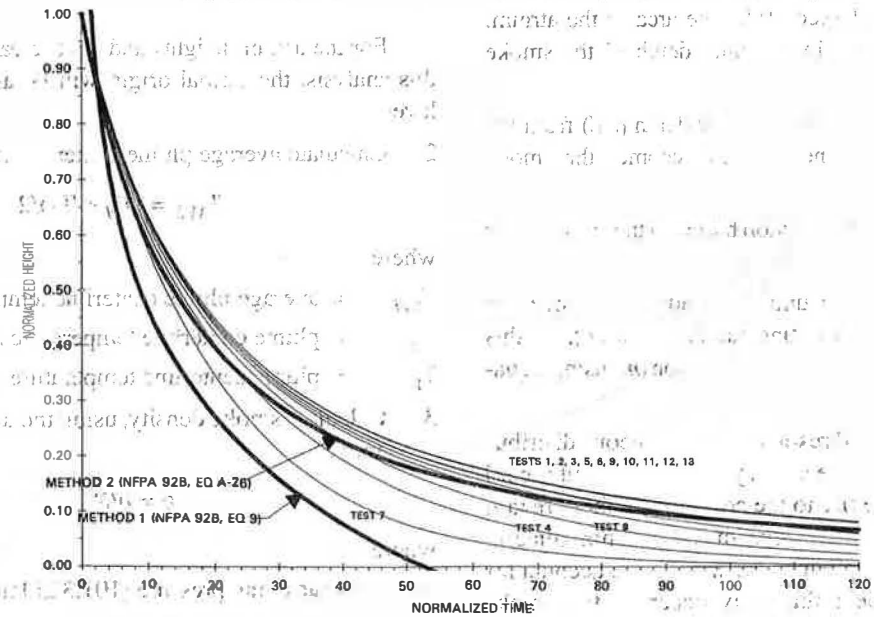

Figure 4 Calculation methods 1, 2, and 3. (Calculation method 3 not adjusted for smoke layer temperature; Method 3 calculations identified by test number.)

clustering of the Method 3 curves around the Method 2 curve. Also note the position of the Method 1 curve. For these calculations, the Method 1 curve represents the fastest predicted filling of the atrium volume.

Figure 5 also illustrates the predicted filling rates, but in this instance, smoke densities have been adjusted based on the calculated average plume temperature. Note the shift of the Method 3 curves toward the origin. Note also that Method 1 no longer predicts the fastest filling of the atriums. Tests 4 and 7 now fall closer to the origin than the Method 1 curve. The Method 2 curve now represents nearly the slowest filling rates.

Figure 6 compares the results from the LES CFD simulations to Methods 1 and 2. The LES CFD results are trendlines derived from the raw data observed from the LES CFD simulations (see Table 2 for LES CFD observed data). The LES CFD simulations show the general distribution of the

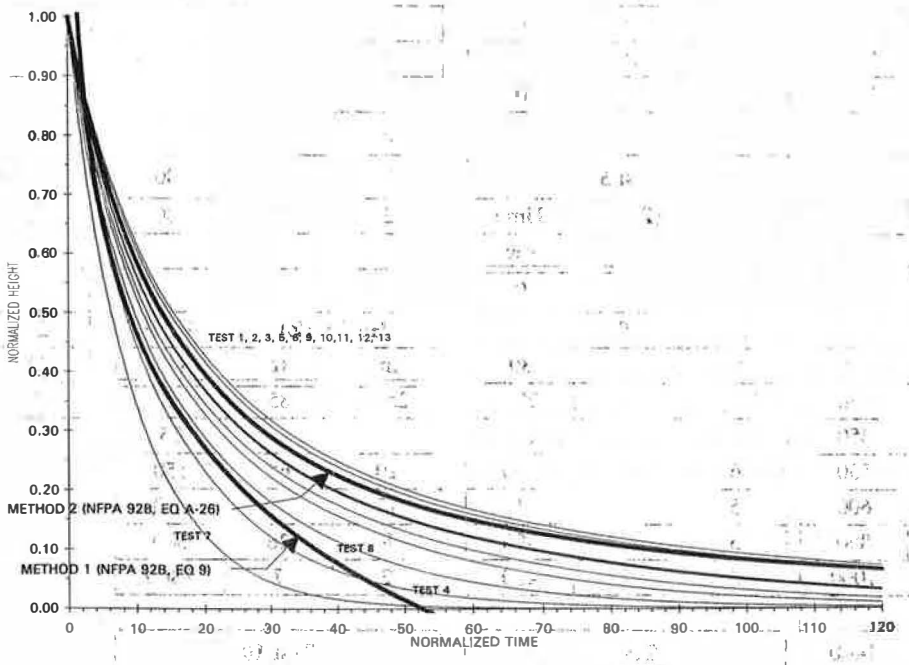

Figure 5 *Calculation methods 1, 2, and 3. (Calculation method 3 adjusted for smoke layer temperature; Method 3 calculations identified by test number.)*

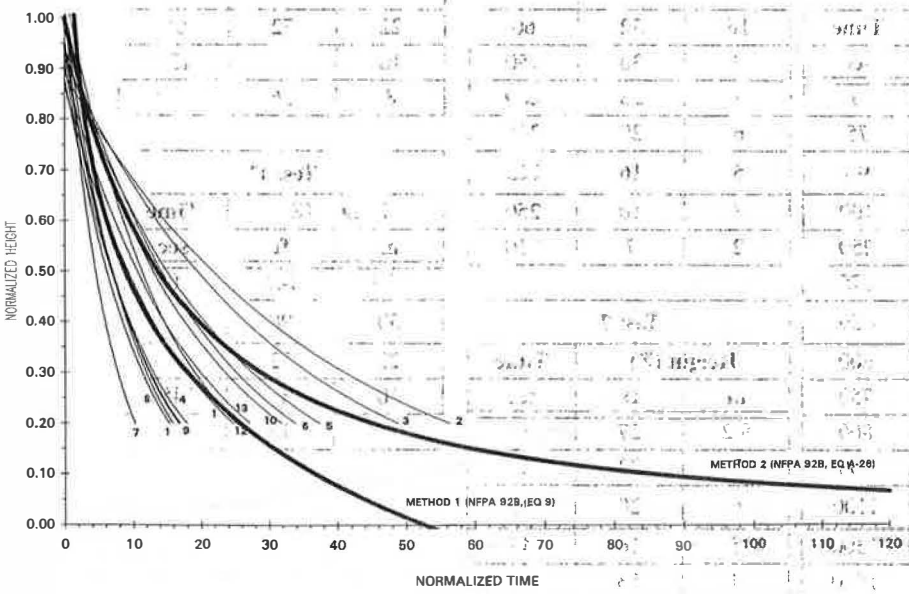

Figure 6 *Calculation methods 1 and 2. (Compared to large eddy simulation CFD predicted curves; LES CFD curves identified by test number.)*

TABLE 2
LES CFD Experimental Observations

Test 1		
Height (Z)		Time
m	ft	sec
30.5	100	0
25	82	200
20	66	280
15	49	500
10	33	1000
7.5	25	1750

Test 2		
Height (Z)		Time
m	ft	sec
101.6	333	0
95	312	75
85	279	110
75	246	130
65	213	350
55	180	550
50	164	600
45	148	850
40	131	1000
35	115	1200
30	98	1400
25	82	1700
20	66	1900

Test 3		
Height (Z)		Time
m	ft	sec
101.6	333	0
95	312	75
85	279	90
75	246	100
65	213	250
55	180	375
50	164	450
45	148	600
40	131	750
35	115	800
30	98	900
25	82	1100
20	66	1300
15	49	1500
10	33	1800

Test 4		
Height (Z)		Time
m	ft	sec
9.6	31	0
7	23	35
6	20	70
5	16	90
3	10	160
2	7	300

Test 5		
Height (Z)		Time
m	ft	sec
32.1	105	0
24	79	30
16	52	80
9	30	220
7	23	280
6	20	290
5	16	310
3	10	400
2	7	450

Test 6		
Height (Z)		Time
m	ft	sec
32.1	105	0
24	79	30
16	52	60
9	30	150
7	23	200
6	20	215
5	16	225
3	10	250
2	7	310

Test 7		
Height (Z)		Time
m	ft	sec
8.2	27	0
7	23	20
6	20	35
5	16	45
4	13	63
3	10	90
2	7	125

Test 8		
Height (Z)		Time
m	ft	sec
18.3	60	0
16	52	25
14	46	50
12	39	125
9	30	250
7	23	400
5	16	500
3	10	700
2	7	900

Test 9		
Height (Z)		Time
m	ft	sec
25.9	85	0
25	82	35
20	66	150
13	43	350
8	26	800
2	7	1800

Test 10		
Height (Z)		Time
m	ft	sec
43.1	141	0
31	102	25
22	72	50
10	33	135
8	26	150

Test 11		
Height (Z)		Time
m	ft	sec
43.1	141	0
30	98	250
22	72	600
10	33	1450
4	13	1825

Test 12		
Height (Z)		Time
m	ft	sec
43.1	141	0
30	98	45
22	72	75
10	33	150
2	7	300

Test 13		
Height (Z)		Time
m	ft	sec
43.1	141	0
30	98	65
22	72	150
11	36	375
2	7	900

simulated filling curves. Note the similarity to the Figure 5 curves in that Method 1 does not predict the fastest filling rate for five of the tests. In fact, the LES CFD results for Test 7 predict filling times that are 50% faster than the Method 1 predictions.

Figures 7 through 10 compare all of the calculation methods by separating the test results into the four selected aspect ratios. On each of the four figures, the LES CFD predictions are shown as individual points. These points are the raw data points reported by the LES CFD observer during the observations of the test simulations.

Figure 7. Methods 1, 2, and 3 approximate the LES CFD calculation from $Z/H = 1.0$ to $Z/H = 0.2$. Method 1 predicts faster filling than the LES CFD observed points, but Methods 2 and 3 predict slower filling rates. Due to the asymptotic nature of the Methods 2 and 3 curves, the predicted smoke layer interface arrival times begin to diverge from the LES CFD calculations below a value of $Z/H = 0.3$. Note the divergence of the Method 2 calculation from the LES CFD observations as Z/H decreases.

Figure 8. The Method 1 calculation again predicts faster filling than the LES CFD observed points. However, as the height of the atrium increases, the Method 1 curve begins to overpredict filling times by a wide margin. For nearly all of the $A/H^2 = 0.9$ cases, the Method 3 predictions produce curves with the proper characteristic shape. Below $Z/H = 0.3$, the Method 3 curve's asymptotic shape begins to differ from the LES CFD observed points. Method 2 represents midpoint values for these six tests. Note the linear nature of the LES CFD observed data as Z/H approaches 0.25 to 0.2. Until this point, Method 2 and Method 3 produce results that are reasonably close to the LES CFD observations.

Please refer to Figure 3, which illustrates the results from a fire experiment in an enclosure very similar in aspect ratio to the 0.9 aspect ratios assessed in this analysis. It would appear that the Figure 3 test most closely approximates Test 5. Note that the Test 5 LES CFD observations are closely approximated by the Method 2 and Method 3 calculations, but the Method 1 calculations predict significantly shorter filling times. The LES CFD observations also reflect the linear nature of the smoke layer interface descent observed in the Yamana/Tanaka experiments.

Figure 9. Only two cases represent aspect ratios of 10. In both cases, Method 1 predicted filling times with reasonable accuracy. Method 2 does not appear to be reliable for these cases. Method 3 compares favorably to Method 1 and the LES CFD in Test 4 but does not predict Test 1 with a similar degree of accuracy.

Figure 10. All of the LES CFD observations depict substantially faster filling than the Method 1 calculations. Method 2 appears to be unsatisfactory and fails to correlate with the LES CFD results for each case. Method 3 predicts the Test 7 filling reasonably adequately, but it overpredicts filling times for the other cases.

ANALYSIS

Although the LES CFD model may not be fully validated based on the number of full-scale fire tests, its predicted results have been used as a comparison to zone model calculation methods provided in NFPA 92B.

It appears that the currently available calculation methods may not be useful over the full range of aspect ratios defined in NFPA 92B. The reasons for this are not known, but the

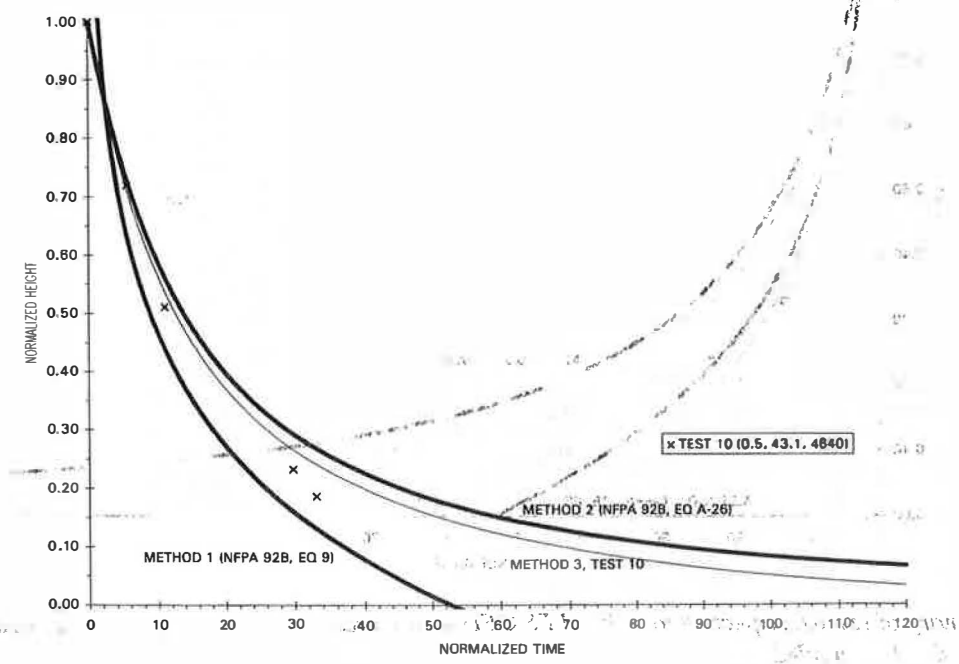

Figure 7 Summary of results. Aspect ratio = 0.5. (LES CFD data represented by individual points.)

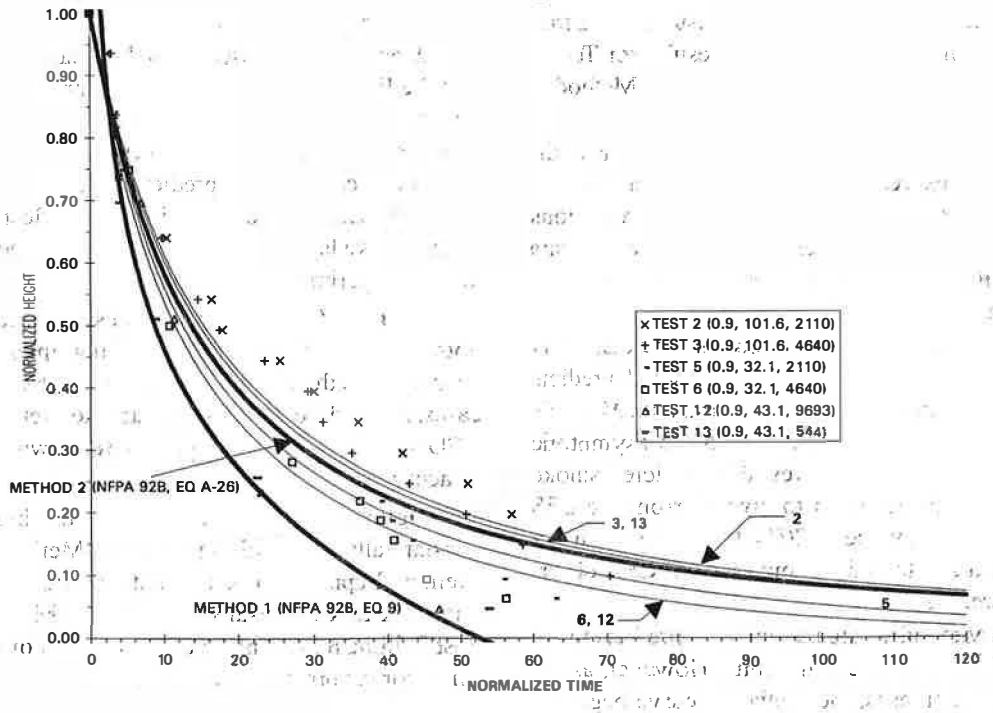

Figure 8 *Summary of results. Aspect ratio = 0.9. (LES CFD data represented by individual points; Method 3 curves individually identified.)*

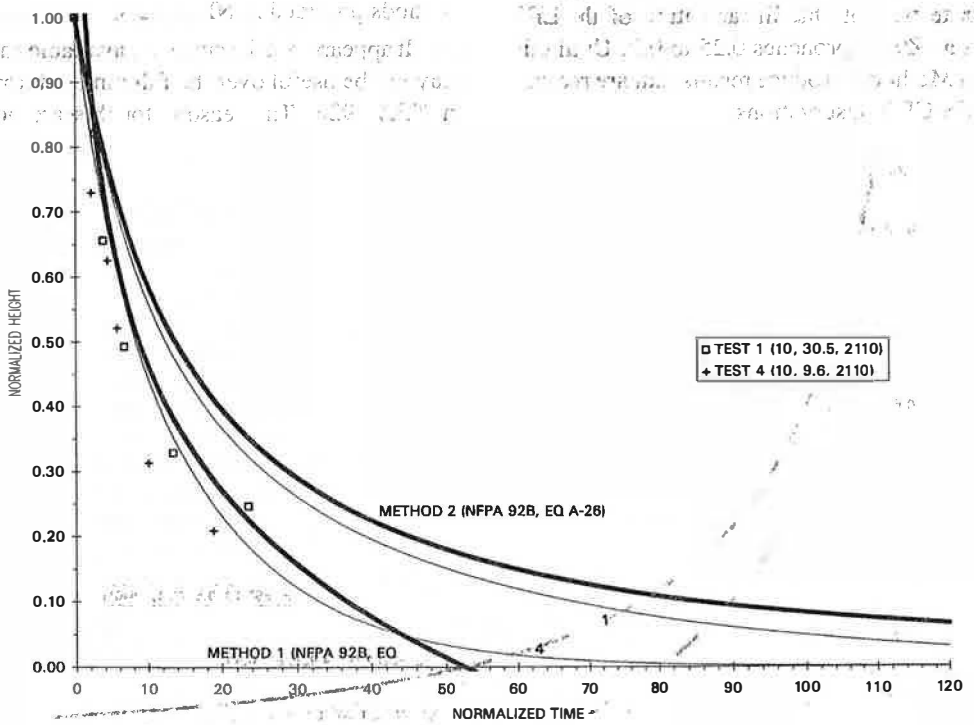

Figure 9 *Summary of results. Aspect ratio = 10. (LES CFD data represented by individual points; Method 3 curves individually identified.)*

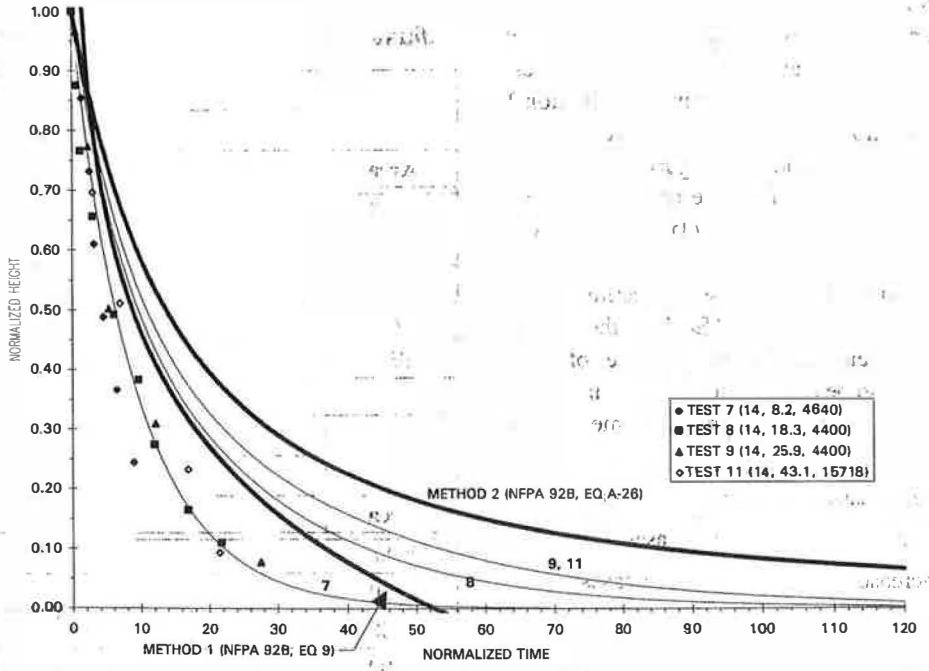

Figure 10 Summary of results. Aspect ratio = 14. (LES CFD points represented by individual points; Method 3 curves individually identified.)

differences are significant for aspect ratios representing the shorter structures (aspect ratio = 14).

Method 1 seems to produce a smoke layer filling curve that exhibits the linear nature of the rate of filling at $Z/H \sim 0.3$ and below. However, it appears that the selection of an initial term of 1.11 limits the usefulness of this method. In some cases, Method 1 overpredicts filling times by a significant margin. In other cases, Method 1 underpredicts filling times by a significant margin.

Figure 11 combines the raw data points from the LES CFD model with a number of curves representing modifications to the initial term of the Equation 1. For reference

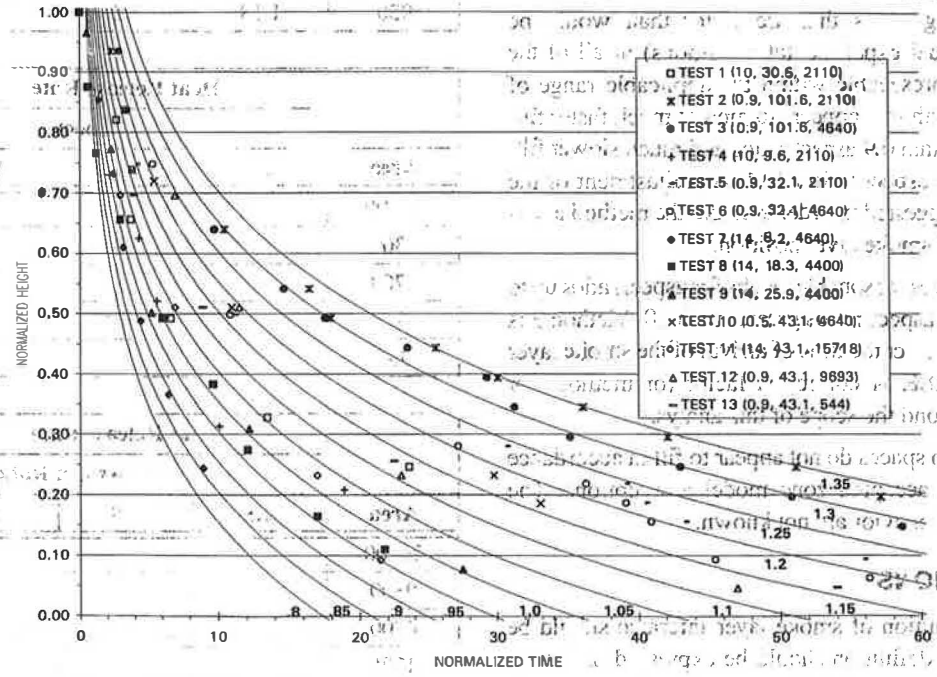

Figure 11 Method 1 curves with adjusted first term vs. LES CFD observations. (LES CFD data points.)

purposes, the curve noted "1.1" approximates the Equation 1 curve. The additional curves represent Equation 1 initial term values from 0.85 to 1.35. Note that each of the LES CFD test observations appear to follow one of the adjusted Equation 1 curves. From this observation, it would appear that the adjustment of the initial term of Equation 1 for a particular combination of aspect ratio, height, and fire size could result in a calculation method that would reflect the observations from the LES CFD experiments.

Table 3 is a presentation of the test cases, separated on the basis of fire size, aspect ratio, and area. Each of the 13 test cases is represented by an entry. Although a number of additional LES CFD tests would be required to provide entries for each configuration and fire size, it appears that some general observations can be made.

1. As the aspect ratio increases, the initial term decreases.
2. As the area increases, the initial term increases.
3. As the fire size increases, the initial term decreases.

CONCLUSIONS

The following conclusions are based on the observed differences between the LES CFD observations and the other calculation methods.

1. Method 2 (NFPA 92B, Equation A-26) is not a reliable predictor of smoke layer position, except for a narrow range of atrium sizes. The results from this equation will likely underpredict filling times by a wide margin using the combinations of heat release rates, heights, and areas in this study.
2. Method 1 (NFPA 92B, Equation 9) does not produce "conservative" results (that is, results that can be relied on to predict filling times that are faster than would be produced in actual experimental conditions) in all of the cases that are foreseeable within the applicable range of aspect ratios. Method 1 appears to predict much faster filling times for certain 0.9 aspect ratios and much slower filling times for an aspect ratio of 14. An adjustment of the initial term is suggested in order to make the method a reliable indicator of smoke layer position.
3. Method 3 produces reasonable results for aspect ratios up to 10. However, at aspect ratios greater than 10, Method 3 is likely to underpredict the time of arrival of the smoke layer interface by 100%. A correction factor (or method) for Method 3 is beyond the scope of this analysis.
4. High aspect ratio spaces do not appear to fill in accordance with previously accepted zone model assumptions. The reasons for this behavior are not known.

RECOMMENDATIONS

1. A standard definition of smoke layer interface should be developed. This definition should be expressed in mathematical terms in order to evaluate (or reevaluate) experimental data previously collected and to evaluate future

TABLE 3
Adjusted Initial Term Values for Method 1 Calculations

	Heat Release Rate			544 kW
	Aspect Ratio			
Area	0.5	0.9	10	14
26000				
9300				
4700		1.13		
1700				
930				

	Heat Release Rate			2110 kW
	Aspect Ratio			
Area	0.5	0.9	10	14
26000				
9300		1.34	1.1	
4700				
1700				
930		1.22		

	Heat Release Rate			4500 kW
	Aspect Ratio			
Area	0.5	0.9	10	14
26000				
9300		1.3		1
4700				0.97
1700				
930	1.18	1.2		0.87

	Heat Release Rate			9700 kW
	Aspect Ratio			
Area	0.5	0.9	10	14
26000				
9300				
4700				
1700		1.12		
930				

	Heat Release Rate			15700 kW
	Aspect Ratio			
Area	0.5	0.9	10	14
26000				0.98
9300				
4700				
1700				
930				

experimental data. The definition would be particularly useful in CFD simulations where mathematic functions are utilized to determine the characteristics of discrete cells in an enclosure.

2. Additional LES CFD simulations would be useful for aspect ratios between 0.9 and 10. The data will be useful to further validate present zone models or can be used to develop improved zone models that can be used for the next several years.

ACKNOWLEDGMENTS

The author would like to thank Mr. Kevin B. McGrattan for his assistance in the preparation of this paper. Mr. McGrattan spent many hours working with definitions, assumptions, and procedures in order to produce the data from the 13 experiments. Without his help, this effort would not have been possible.

REFERENCES

BOCA. 1996. *1996 BOCA National Building Code*. Country Club Hills, Ill.: Building Officials and Code Administrators International, Inc.

BOCA. 1993. *The BOCA National Building Code/1993, Commentary Volume 1*. Country Club Hills, Ill.: Building Officials and Code Administrators International, Inc.

Brooks, W.N. 1997. Comparison of "regular" and "irregular" methods of calculating smoke layer interface heights in 1996 BOCA National Building Code. *ASHRAE Transactions* 103(2): 554-568.

Chow, W.K. 1995. A comparison of the use of fire zone and field models for simulating atrium smoke filling processes. *Fire Safety Journal* 25: 337-353.

He, Y., P. Fernando, and A. Luo. 1998. Determination of interface height from measured parameter profile in enclosure fire experiment. *Fire Safety Journal*, 31(1): 19-38.

ICBO. 1997. *Uniform building code*. Whittier, Calif.: International Conference of Building Officials.

Klote, J.H. 1994. Equation 10, Method of predicting smoke movement in atria with application to smoke management. NISTIR 5516, Building and Fire Research Laboratory, National Institute of Standards and Technology, Gaithersburg, Md.

McGrattan, K.B., H.R. Baum, and R.G. Rehm. 1998. Large eddy simulations of smoke movement. *Fire Safety Journal*, 30: 161-178.

McGrattan, K.B., H.R. Baum, and R.G. Rehm. 1997. Large eddy simulations of fire experiments. *ASME Heat Transfer Conference Proceedings*.

NFPA. 1995. NFPA *Standard 92B, Guide for smoke management systems in atria, covered malls, and large areas*. Quincy, Mass.: National Fire Protection Association.

NFPA. 1997. *NFPA Standard 101, Life Safety Code*. Quincy, Mass.: National Fire Protection Association.

Söderbom, J. 1992. Smoke spread experiments in large rooms. Experimental results and numerical simulations. Swedish National Testing and Research Institute Fire Technology SP Report 1992:52.

Yamana, T., and T, Tanaka. 1985. Smoke control in large scale spaces, Part 2: Smoke control experiments in a large scale space. *Fire Science and Technology* 5(1):41-54.